Frontiers of Information Technology & Electronic Engineering
www.jzus.zju.edu.cn; engineering.cae.cn; www.springerlink.com
ISSN 2095-9184 (print); ISSN 2095-9230 (online)
E-mail: jzus@zju.edu.cn

An effective approach for low-complexity maximum likelihood based automatic modulation classification of STBC-MIMO systems*

Maqsood H. SHAH‡, Xiao-yu DANG

College of Electronic and Information Engineering, Nanjing University of Aeronautics and Astronautics, Nanjing 211106, China

E-mail: maqsood@nuaa.edu.cn; dang@nuaa.edu.cn

Received May 16, 2018; Revision accepted Sept. 24, 2018; Crosschecked Oct. 10, 2019; Published online Dec. 27, 2019

Abstract: A low-complexity likelihood methodology is proposed for automatic modulation classification of orthogonal space-time block code (STBC) based multiple-input multiple-output (MIMO) systems. We exploit the zero-forcing equalization technique to modify the typical average likelihood ratio test (ALRT) function. The proposed ALRT function has a low computational complexity compared to existing ALRT functions for MIMO systems classification. The proposed approach is analyzed for blind channel scenarios when the receiver has imperfect channel state information (CSI). Performance analysis is carried out for scenarios with different numbers of antennas. Alamouti-STBC systems with 2×2 and 2×1 and space-time transmit diversity with a 4×4 transmit and receive antenna configuration are considered to verify the proposed approach. Some popular modulation schemes are used as the modulation test pool. Monte-Carlo simulations are performed to evaluate the proposed methodology, using the probability of correct classification as the criterion. Simulation results show that the proposed approach has high classification accuracy at low signal-to-noise ratios and exhibits robust behavior against high CSI estimation error variance.

Key words: Multiple-input multiple-output; Space-time block code; Maximum likelihood; Automatic modulation classification; Zero-forcing

https://doi.org/10.1631/FITEE.1800306 **CLC number:** TP391.4

1 Introduction

Study on automatic modulation classification (AMC) has its roots in the military requirements for electronic warfare operations, such as spectrum surveillance and communication intelligence. However, with the emergence of software-defined radio (SDR) and cognitive radio in the last couple of decades, AMC has found significance for civilian applications. For example, AMC can be used to avoid interference in a congested radio environment. A transmission unit can tune its parameters on the basis of a classified modulation in an adjacent channel, and keep the interference to the minimum. In the case of SDR, where overhead data is transmitted along with the main payload for reconfiguration, AMC can be used to optimize the transmission efficiency (Bahloul et al., 2016).

A lot of work has been done with regard to AMC for single-input and single-output (SISO) systems (Dobre et al., 2007). With the emergence of multiple-input multiple-output (MIMO) systems, which tackle the modern requirements of high data rates and reliability in multi-path fading

‡ Corresponding author

* Project supported by the National Natural Science Foundation of China (Nos. 61172078, 61571224, and 61571225) and Six Talent Peaks Project in Jiangsu Province, China

ORCID: Maqsood H. SHAH, http://orcid.org/0000-0002-7375-0131

environments, the problem of AMC poses new challenges. Space-time block code (STBC) is a methodology in the context of MIMO systems, sending multiple copies of the desired signal for high reliability transmission. Many variants of this technique have been proposed (Alamouti, 1998; Tarokh et al., 1999). More recently, STBC-MIMO has found its application in optical wireless communications. A robust method based on Alamouti-STBC (Al-STBC) was proposed which can perform well under turbulent atmospheric conditions (Niu et al., 2014; Thao et al., 2016). In the context of power line communication networks, different variants of STBC have been used to achieve enhanced performance (Quan and Ribeiro, 2011; Tseng et al., 2017). STBC has also been used in cooperative relay scenarios to achieve high data rates. Veljovic and Urosevic (2017) used orthogonal STBC (OSTBC) with a configuration of 4×1 to achieve $3/4$ data rate. Similarly, a distributed quasi OSTBC was used to achieve better bit-error-rate performance (Tseng and Liao, 2014).

There are different MIMO techniques which are still evolving with contemporary developments in the field of communications. AMC for MIMO systems is still a very active research area. There are two broader categories for modulation classification algorithms, decision-theoretic (or likelihood-based) (Huang and Polydoros, 1995; Sills, 1999; Wei and Mendel, 2000) and pattern recognition (or feature-based) (Nandi and Azzouz, 1997, 1998; Swami and Sadler, 2000). The likelihood-based approach is a probabilistic solution and performs optimal classification in the Bayesian sense. It is based on prior knowledge of the probability distribution and hypothesis (Sills, 1999). The feature-based approach depends on some basic features (or characteristics) of a received signal (Nandi and Azzouz, 1997). There are two broader categories to solve the classification problem after obtaining the feature set, hierarchical tree based (Swami and Sadler, 2000) and machine learning based approaches. The support vector machine (Zhu et al., 2011), k-nearest neighbor (Aslam et al., 2012), and artificial neural network (Nandi and Azzouz, 1998) are some of the machine learning based modulation classifiers. Recently, evolution of deep learning for pattern recognition has inspired work in the field of communications. Ali and Fan (2017) used deep learning to perform modulation classification without explicit extraction of a feature set. However, most of the AMC work in deep learning still pertains to SISO systems.

Eldemerdash et al. (2013) proposed a feature-based approach for modulation classification of Al-STBC systems. For spatially correlated MIMO systems, a feature-based approach using higher-order moments and cumulants was proposed in Hassan et al. (2010). Some other feature-based (Shi et al., 2007; Mühlhaus et al., 2012; Marey and Dobre, 2015) and maximum likelihood (ML) based methodologies (Choqueuse et al., 2010; Luo et al., 2012; Salam et al., 2015; Turan et al., 2016) have been proposed for AMC of different MIMO systems. The computational complexity of likelihood functions proposed in these studies increases with the increase of the number of antennas, which makes them less practical for higher numbers of antennas in real-time scenarios.

In this study, we propose an ML-based modulation classification approach for OSTBC-MIMO systems. We exploit the zero-forcing (ZF) equalization technique to achieve a consequential low-complexity solution. An updated ALRT function, independent of the antenna number, is proposed using the ZF-equalized symbols for classification. The impact of the CSI estimation error (Beres and Adve, 2007) on modulation classification is simulated and discussed. The proposed algorithm has been verified for the Al-STBC system with 2×2 and 2×1 and space-time transmit diversity (STTD) with a 4×4 transmit and receive antenna configuration. The probability of correct classification is used as the performance criterion. Simulations reveal high classification accuracy at a practical signal-to-noise ratio (SNR) range and CSI estimation error variance.

2 System model

In this section the general flow of the overall classification process is explained briefly. Fig. 1 depicts an overall flow diagram of our system model. In the radio frequency preprocessing block, the signal received by N_{r} antennas is mixed with a correlated channel matrix and subsequently provided as input to the ZF equalization block after addition of additive white Gaussian noise (AWGN). Typical ML-based modulation classification methodologies consider non-equalized symbols at multiple receive antennas. In this study, we use the symbols after ZF equalization for ML-based classification.

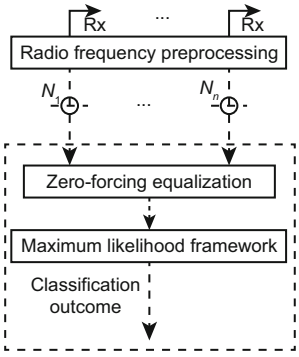

Fig. 1 Overall process flow diagram of the proposed study

For a MIMO system with N_t transmit antennas and N_r receive antennas, the received signal vector is given by

$$\boldsymbol{R}=\boldsymbol{H}\boldsymbol{S}+\boldsymbol{N}, \tag{1}$$

where $\boldsymbol{R}$ is the receive data vector, $\boldsymbol{H}$ is the block-fading channel with Rayleigh distribution, $\boldsymbol{S}$ is the transmitted vector consisting of modulated symbols, and $\boldsymbol{N}$ is the AWGN channel vector with variance σ_n^2.

The signal model for Al-STBC $(2\times 2, 2\times 1)$ and for STTD (4×4) transmit and receive antenna configurations is further explained in the following subsections.

2.1 Al-STBC with 2 × 2 MIMO configuration

Alamouti block coding is a transmit diversity technique which can be used in the 2×1 multiple-input and single-output (MISO) and 2×2 MIMO configurations (Alamouti, 1998). We consider the 2×2 MIMO configuration to elaborate the signal model and achieve a generalized received signal vector form. Table 1 represents the Al-STBC scheme, where s_{2k+1} and s_{2k+2} are symbols transmitted by antennas 1 and 2 at time slot $2k+1$, respectively. Similarly, $-s_{2k+2}^*$ and s_{2k+1}^* are symbols transmitted by antennas 1 and 2 at time slot $2k+2$, respectively, where * represents the conjugate, $k\in 0,1,\ldots,L/2$, and L is the block length of data symbols. The process of received vector combination for multiple antennas at different time slots is elaborated for the 2×2 Al-STBC configuration, which is subsequently generalized for other scenarios.

Table 1 Al-STBC code

Antenna	Time slot	
	$2k+1$	$2k+2$
1	s_{2k+1}	$-s_{2k+2}^*$
2	s_{2k+2}	s_{2k+1}^*

The received signals for antennas 1 and 2 at time slot $2k+1$ are given by

$$\overset{(2k+1)}{r_1}=h_{11}s_{2k+1}+h_{12}s_{2k+2}+\overset{(2k+1)}{n_1}, \tag{2}$$

$$\overset{(2k+1)}{r_2}=h_{21}s_{2k+1}+h_{22}s_{2k+2}+\overset{(2k+1)}{n_2}. \tag{3}$$

In Eqs. (2) and (3), overset is used to denote the time slot and the subscript emphasizes the antenna number. The received signals for antennas 1 and 2 at time slot $2k+2$ can be given by

$$\overset{(2k+2)}{r_1}=h_{11}(-s_{2k+2}^*)+h_{12}s_{2k+1}^*+\overset{(2k+2)}{n_1}, \tag{4}$$

$$\overset{(2k+2)}{r_2}=h_{21}(-s_{2k+2}^*)+h_{22}s_{2k+1}^*+\overset{(2k+2)}{n_2}. \tag{5}$$

By taking the conjugate of Eqs. (4) and (5) and rearranging to obtain a combined received vector for both antennas at time slots $2k+1$ and $2k+2$, we have

$$\overset{(2k+1)}{\boldsymbol{R}}=\begin{bmatrix}\overset{(2k+1)}{r_1}\\ \overset{(2k+1)}{r_2}\end{bmatrix}=\begin{bmatrix}h_{11} & h_{12}\\ h_{21} & h_{22}\end{bmatrix}\begin{bmatrix}s_{2k+1}\\ s_{2k+2}\end{bmatrix}+\begin{bmatrix}\overset{(2k+1)}{n_1}\\ \overset{(2k+1)}{n_2}\end{bmatrix}, \tag{6}$$

$$\overset{(2k+2)}{\boldsymbol{R}}=\begin{bmatrix}\overset{(2k+2)}{r_1^*}\\ \overset{(2k+2)}{r_2^*}\end{bmatrix}=\begin{bmatrix}h_{12}^* & -h_{11}^*\\ h_{22}^* & -h_{21}^*\end{bmatrix}\begin{bmatrix}s_{2k+1}\\ s_{2k+2}\end{bmatrix}+\begin{bmatrix}\overset{(2k+2)}{n_1^*}\\ \overset{(2k+2)}{n_2^*}\end{bmatrix}. \tag{7}$$

By combining the received vectors for different time slots in Eqs. (6) and (7), we have

$$\overleftrightarrow{\boldsymbol{R}}=\overleftrightarrow{\boldsymbol{H}}\boldsymbol{S}+\overleftrightarrow{\boldsymbol{N}}, \tag{8}$$

where $\leftrightarrow$ represents the concatenation operation, $\overleftrightarrow{\boldsymbol{R}}=\begin{bmatrix}\overset{(2k+1)}{\boldsymbol{R}}\\ \overset{(2k+2)}{\boldsymbol{R}}\end{bmatrix}$, $\overleftrightarrow{\boldsymbol{H}}=\begin{bmatrix}\overset{(2k+1)}{\boldsymbol{H}}\\ \overset{(2k+2)}{\boldsymbol{H}}\end{bmatrix}$, and $\overleftrightarrow{\boldsymbol{N}}=\begin{bmatrix}\overset{(2k+1)}{\boldsymbol{N}}\\ \overset{(2k+2)}{\boldsymbol{N}}\end{bmatrix}$.

2.2 STTD with 4 × 4 MIMO configuration

The space-time code for four antennas, using STTD and orthogonal transmit diversity (OTD), was defined by Jalloul et al. (1999). Table 2 shows the STBC for four transmit antennas.

Following a similar process for 2×2 Al-STBC as in the previous subsection, we can write the combined received vector for the 4×4 STBC-MIMO configuration as

Table 2 Orthogonal STTD-OTD code

Antenna	Time slot			
	$4k+1$	$4k+2$	$4k+3$	$4k+4$
1	s_{4k+1}	$-s^*_{4k+2}$	s_{4k+1}	$-s^*_{4k+2}$
2	s_{4k+2}	s^*_{4k+1}	s_{4k+2}	s^*_{4k+1}
3	s_{4k+3}	$-s^*_{4k+4}$	$-s_{4k+3}$	s^*_{4k+4}
4	s_{4k+4}	s^*_{4k+3}	$-s_{4k+3}$	$-s^*_{4k+3}$

$$\overleftrightarrow{\boldsymbol{R}}=\begin{bmatrix}^{(4k+1)}\\ \boldsymbol{R}\\ ^{(4k+2)}\\ \boldsymbol{R}\\ ^{(4k+3)}\\ \boldsymbol{R}\\ ^{(4k+4)}\\ \boldsymbol{R}\end{bmatrix}=\begin{bmatrix}^{(4k+1)}\\ \boldsymbol{H}\\ ^{(4k+2)}\\ \boldsymbol{H}\\ ^{(4k+3)}\\ \boldsymbol{H}\\ ^{(4k+4)}\\ \boldsymbol{H}\end{bmatrix}\begin{bmatrix}s_{4k+1}\\ s_{4k+2}\\ s_{4k+3}\\ s_{4k+4}\end{bmatrix}+\begin{bmatrix}^{(4k+1)}\\ \boldsymbol{N}\\ ^{(4k+2)}\\ \boldsymbol{N}\\ ^{(4k+3)}\\ \boldsymbol{N}\\ ^{(4k+4)}\\ \boldsymbol{N}\end{bmatrix}. \tag{9}$$

The generalized form for the combined received vector for multiple antennas and time slots is thus given by

$$\overleftrightarrow{\boldsymbol{R}}_{(N_\mathrm{t}N_\mathrm{r}\times 1)}=\overleftrightarrow{\boldsymbol{H}}_{(N_\mathrm{t}N_\mathrm{r}\times N_\mathrm{t})}\boldsymbol{S}_{(N_\mathrm{t}\times 1)}+\overleftrightarrow{\boldsymbol{N}}_{(N_\mathrm{t}N_\mathrm{r}\times 1)}. \tag{10}$$

The combined channel matrix $\overleftrightarrow{\boldsymbol{H}}$ depends on the number of receive antennas N_r and orthogonal code. The subscripts in Eq. (10) represent the dimension of vectors.

3 Channel estimation model and zero-forcing equalization

3.1 CSI estimation error model

For the full-blind classification scenario, the CSI matrix has to be estimated before applying ZF equalization (Beres and Adve, 2007). We do not perform CSI estimation in our study. However, we model the estimated channel to investigate the effect of the estimation error in our proposed methodology. Eq. (11) represents the modeled estimated channel $\hat{\boldsymbol{H}}$:

$$\hat{\boldsymbol{H}}=\boldsymbol{H}+\sigma_\mathrm{e}^2\boldsymbol{\alpha}, \tag{11}$$

where $\hat{\boldsymbol{H}}$ is the estimated channel matrix, σ_e^2 is the variance of the channel estimation error, and $\boldsymbol{\alpha}$ is the matrix of the same size as $\boldsymbol{H}$ and has the entries (zero-mean and unit variance) which are independent and identically distributed (i.i.d.) random variables with a standard normal distribution.

3.2 Zero-forcing equalization

ZF equalization uses the inverse of a channel response to recover the equalized symbols. Once symbols of block length L are received at multiple receive antennas, we use the ZF equalization method to obtain the equalized symbols, which are then passed on as input to the ML framework for modulation classification. Eq. (10) shows the generalized combined received signals for multiple time slots at different receive antennas. We need to solve Eq. (10) for vector $\boldsymbol{S}$. The pseudo-inverse of a matrix is defined by $\boldsymbol{H}^\dagger=(\boldsymbol{H}^\mathrm{H}\boldsymbol{H})^{-1}\boldsymbol{H}^\mathrm{H}$ (Ben-Israel and Greville, 2003). Equation for the equalized symbol vector $\hat{\boldsymbol{S}}$ is thus given by

$$\hat{\boldsymbol{S}}=\boldsymbol{H}^\dagger(\boldsymbol{H}\boldsymbol{S}+\boldsymbol{N}), \tag{12}$$

$$\hat{\boldsymbol{S}}=\boldsymbol{S}+\boldsymbol{H}^\dagger\boldsymbol{N}\simeq\boldsymbol{S}+((\boldsymbol{H}^\mathrm{H}\boldsymbol{H})^{-1}\boldsymbol{H}^\mathrm{H})\boldsymbol{N}, \tag{13}$$

where † denotes the pseudo-inverse and ∧ emphasizes the equalized received symbols. Finally, for the block of length L, the equalized symbol vector $\hat{\boldsymbol{S}}$ is concatenated and used in the ML framework for modulation classification.

4 Proposed maximum likelihood framework

A decision-theoretic based approach for modulation classification is based on the ML works of the principle of hypothesis testing for multiple unknowns (Sills, 1999). We represent our likelihood function for a certain modulation ψ by $\Lambda(\boldsymbol{R}|\psi,\boldsymbol{H})$, where $\boldsymbol{R}$ is the received signal vector, ψ represents the modulation format, and $\boldsymbol{H}$ is the channel coefficient matrix for a flat-fading Rayleigh channel. In the context of the ML framework, the most probable classified modulation is the one that maximizes the above likelihood function (Choqueuse et al., 2010; Luo et al., 2012), such that

$$\hat{\psi}=\underset{\psi\in\Theta}{\operatorname{argmax}}(\Lambda(\boldsymbol{R}|\psi,\boldsymbol{H})), \tag{14}$$

where $\hat{\psi}$ denotes the classified modulation and $\Theta=\{\psi_1,\psi_2,\ldots,\psi_n\}$ represents the modulation pool for which the likelihood function is maximized. In our case, some popular modulation schemes, including binary phase shift keying (BPSK), quadrature phase shift keying (QPSK), 8 phase shift keying (8PSK), and 16 quadrature amplitude modulation (16QAM), are used as the modulation test pool.

$\Theta = (\psi_1 = \text{BPSK}, \psi_2 = \text{QPSK}, \psi_3 = \text{8PSK}, \psi_4 = \text{16QAM})$. A likelihood function depends on certain random variables. In our case, transmitted symbols S and Gaussian noise are the intrinsic random variables. ALRT is the optimal solution in the Bayesian sense, as given by Choqueuse et al. (2010).

$$\Lambda(\boldsymbol{R}|\psi, \boldsymbol{H}) = \int_S \Lambda(\boldsymbol{R}|\psi, S, \boldsymbol{H}) P[S/\psi] \mathrm{d}S, \quad (15)$$

where S is the transmitted symbol corresponding to modulation under test and $P[S/\psi]$ is the probability of S under modulation ψ. Since we assume that transmitted symbols are i.i.d. random variables, we can rewrite Eq. (15) as

$$\Lambda(\boldsymbol{R}|\psi, \boldsymbol{H}) = \prod_{k=1}^{L} \int_{S(k)} \Lambda(\boldsymbol{R}(k)|\psi, S(k), \boldsymbol{H}) P[S(k)/\psi] \mathrm{d}S. \quad (16)$$

Since $P[S(k)/\psi]$ is equal to $1/(M^{N_\mathrm{t}})$, where M is the number of constellation points and N_t is the number of transmit antennas, Eq. (16) can be rewritten as

$$\Lambda(\boldsymbol{R}|\psi, \boldsymbol{H}) = \frac{1}{M^{L \cdot N_\mathrm{t}}} \prod_{k=1}^{L} \sum_{S(k) \in \psi^{N_\mathrm{t}}} \Lambda(\boldsymbol{R}(k)|\psi, S(k), \boldsymbol{H}). \quad (17)$$

For a received signal $\boldsymbol{R}(k)$ given the channel matrix $\boldsymbol{H}$ and noise variance σ_n^2, the probability density function is given by

$$\Lambda(\boldsymbol{R}(k)|S(k), \boldsymbol{H}) = \frac{1}{(\pi\sigma_\mathrm{n}^2)^{N_\mathrm{r}}} \exp\left(-\frac{1}{\sigma_\mathrm{n}^2} ||\boldsymbol{R}(k) - \boldsymbol{H}S(k)||_\mathrm{F}^2\right). \quad (18)$$

Substituting Eq. (17) into Eq. (16), we have

$$\Lambda(r|\psi, \boldsymbol{H}) = \frac{1}{(M^{L \cdot N_\mathrm{t}})(\pi\sigma_\mathrm{n}^2)^{N_\mathrm{r}}} \prod_{k=1}^{L} \sum_{S(k) \in \psi^{N_\mathrm{t}}} \exp\left[-\frac{1}{\sigma_\mathrm{n}^2} ||\boldsymbol{R}(k) - \boldsymbol{H}S(k)||_\mathrm{F}^2\right]. \quad (19)$$

Maximizing Eq. (19) can give us the desired classification results. However, for ease of analysis, the log likelihood function of Eq. (19) is used instead:

$$\log(\Lambda(\boldsymbol{R}|\psi, \mathrm{H})) = -LN_\mathrm{t} \log M - N_\mathrm{r} \log(\pi\sigma_\mathrm{n}^2) + \sum_{k=1}^{L} \log\left(\sum_{S(k) \in \psi^{N_\mathrm{t}}} \exp\left(-\frac{||\boldsymbol{R}(k) - \boldsymbol{H}S(k)||_\mathrm{F}^2}{\sigma_\mathrm{n}^2}\right)\right). \quad (20)$$

In Eq. (20), L is the block length of symbols, $\boldsymbol{H}$ is the channel matrix, N_t and N_r are the numbers of transmit and receive antennas respectively, σ_n^2 is the noise variance, and M is the number of constellation points corresponding to hypothesis ψ.

It is evident from Eq. (20) that the computational complexity of the log likelihood function increases with the increasing number of transmitters. For Al-STBC and STTD-OTD MIMO schemes discussed in the previous section, we propose a different approach to use this ALRT function, which gets rid of this additional complexity due to the increasing number of transmitters. Instead of using the received vector $\boldsymbol{R}$ at different antennas, we use the equalized symbol vector $\hat{\boldsymbol{S}}$ derived in Eq. (12) for ML estimation. The updated low-complexity ALRT function is accordingly given by

$$\log(\Lambda(\hat{\boldsymbol{S}}|\psi, \boldsymbol{H})) = -L \log M - \log(\pi\sigma_\mathrm{n}^2) + \sum_{k=1}^{L} \log\left(\sum_{S(k) \in \psi} \exp\left[-\frac{||\hat{\boldsymbol{S}} - S(k)||_\mathrm{F}^2}{\sigma_\mathrm{n}^2}\right]\right). \quad (21)$$

This function is evaluated via Monte-Carlo simulations for three different scenarios of OSTBC-MIMO systems, which are discussed in Section 5.

The proposed ALRT function in Eq. (21) is independent of the number of transmit antennas (N_t) or receive antennas (N_r). A typical ALRT function for a MIMO system (Choqueuse et al., 2009; Luo et al., 2012) as given in Eq. (20) has exponential operations of order $(MN)^{N_\mathrm{t}}$, where M is the order of the modulation scheme, N is the number of samples, and N_t is the number of transmit antennas. Our proposed methodology manages to get rid of the additional complexity of order $O(N_\mathrm{t})$ caused by the additional number of antennas and has exponential operations of order MN similar to that of a SISO system. In the case of a full-blind classification scenario, the channel matrix $\boldsymbol{H}$ has to be estimated before the ZF equalization stage and the proposed ALRT function is also independent of $\boldsymbol{H}$.

We achieve ZF equalization using Moore-Penrose pseudo-inverse (Ben-Israel and Greville, 2003). Pseudo-inverse has been used in very diverse areas and a lot of work has been done to optimize its complexity (Courrieu, 2008; Saurabh, 2015). The built-in MATLAB function that we used to carry out simulations is based on spectral value decomposition. In general, the complexity of a pseudo-inverse

is of order $O(n^{\omega})$ (Cormen et al., 2009), where n is the matrix dimension and ω is the matrix multiplication constant with an upper bound of 2.372 863 9 (Le Gall, 2016).

5 Simulation results

The performance of the proposed algorithm is evaluated in this section. Five hundred Monte-Carlo iterations were performed for each modulation hypothesis (ψ_i) among a modulation pool of BPSK, QPSK, 8PSK, and 16QAM. The Al-STBC MIMO system with 2×2 and 2×1 and STTD-OTD with a 4×4 antenna configuration were considered for verification of the proposed algorithm. Classification performance for each system was evaluated with and without consideration of the perfect CSI knowledge. An SNR range of -15 to 15 dB with 1 dB increment and CSI estimation error variance $\sigma_{\mathrm{e}}^2=\{0,0.1,0.3\}$ were considered for performance evaluation. For ease of graphical visualization, the P_{cc} of modulations other than the hypothesis (or falsely classified modulations) were averaged for different values of σ_{e}^2 such that

$$\mathrm{Avg}P_{\mathrm{cc}}(\psi_i|\psi_j)=\frac{1}{3}\sum_{n=1}^{3}P_{\mathrm{cc}}(\psi_i|\psi_j)|(\sigma_{\mathrm{e}}^2(n)), \quad (22)$$

where $i\neq j$, $\sigma_{\mathrm{e}}^2(1)=0$ when the receiver has perfect CSI knowledge, $\sigma_{\mathrm{e}}^2(2)=0.1$, and $\sigma_{\mathrm{e}}^2(3)=0.3$. Simulation results for three different configurations are discussed separately in subsequent subsections.

5.1 Performance of 2×1 Al-STBC

All simulations were carried out for a length of $L=1024$ i.i.d. modulated symbols. The signal power and modulation type from all the transmit antennas were assumed to be the same, and the number of transmit antennas N_{t} and noise variance σ_{n}^2 were known at the receiver. Fig. 2 shows the classification results for Al-STBC for the 2×1 antenna configuration. Figs. 2a–2d show the percentage of correct classification when BPSK, QPSK, 8PSK, and 16QAM were transmitted. When $\sigma_{\mathrm{e}}^2=0$ (with perfect CSI knowledge), 100% classification results were achieved at almost 5 dB and beyond for all hypotheses. In the case of imperfect CSI, when $\sigma_{\mathrm{e}}^2=0.1$, 90% correct classification was achieved at 5 dB and beyond for BPSK, QPSK, and 16QAM and at 0 dB for 8PSK. When $\sigma_{\mathrm{e}}^2=0.3$, more than 70% correct classification was achieved at 5 dB for BPSK and QPSK and at 0 dB for 16QAM. For 8PSK, 90% correct classification was achieved at 5 dB and beyond when $\sigma_{\mathrm{e}}^2=0.3$.

5.2 Performance of 2×2 Al-STBC

Classification results for Al-STBC with a 2×2 antenna configuration are depicted in Fig. 3. As expected, the performance has been significantly improved compared to the 2×1 MISO scenario. Fig. 3a shows the percentage of correct classification when BPSK was transmitted. When $\sigma_{\mathrm{e}}^2=0$, 100% correct classification was achieved at -3 dB and beyond. In the case of imperfect CSI , when σ_{e}^2 was 0.1, more than 90% correct classification was achieved at 0 dB and beyond. However, when $\sigma_{\mathrm{e}}^2=0.3$, more than 80% correct classification was achieved at 0 dB and beyond. Similar results can be deduced from Figs. 3b–3d, which show the correct classification percentage for QPSK, 8PSK, and 16QAM transmissions. With perfect CSI knowledge, QPSK, 8PSK, and 16QAM transmissions all achieved 100% correct classification at -3 dB and beyond. When $\sigma_{\mathrm{e}}^2=0.1$, QPSK, 8PSK, and 16QAM achieved at least 90% correct classification at -2, -5, and -2 dB, respectively. In the case of $\sigma_{\mathrm{e}}^2=0.3$, 90% correct classification was achieved at 0 dB for QPSK and 16QAM and at -5 dB for 8PSK.

5.3 Performance of 4×4 STTD-OTD

The classification results for 4×4 STTD-OTD are shown in Fig. 4. It is evident from Figs 4a–4d that a perfect classification in the case of $\sigma_{\mathrm{e}}^2=0$ was achieved at -9, -8, -5, and -8 dB for BPSK, QPSK, 8PSK, and 16QAM, respectively. When $\sigma_{\mathrm{e}}^2=0.1$ and 0.3, more than 90% correct classification was achieved at -5 dB and beyond.

It can be generalized in view of the above simulation results for all the three presented scenarios that classification performance increases with the increasing number of receive antennas. The best results were achieved in the 4×4 antenna configuration. When a channel estimation error variance σ_{e}^2 was up to 0.3, the results for 2 and 4 antennas were very promising with almost 90% correct classification at less than -5 dB.

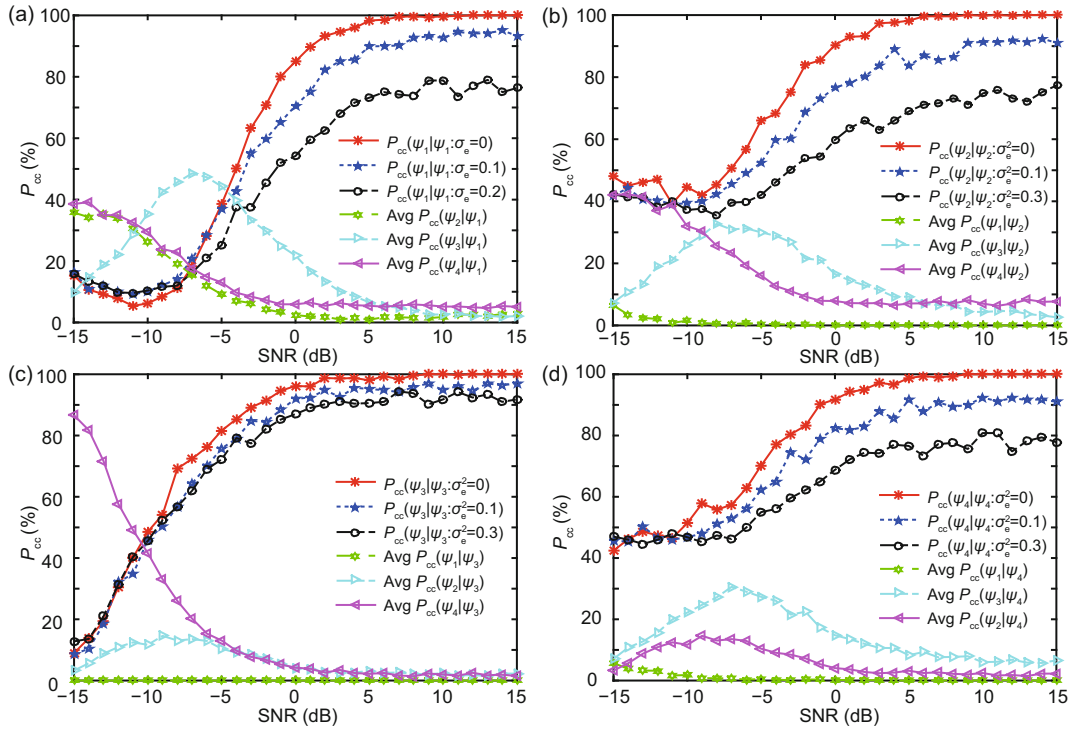

Fig. 2 Classification performance of 2×1 Al-STBC MISO for $\psi_1 =$ BPSK (a), $\psi_2 =$ QPSK (b), $\psi_3 =$ 8PSK (c), and $\psi_4 =$ 16QAM (d) with $L = 1024$ symbols at different CSI estimation error values σ_e^2

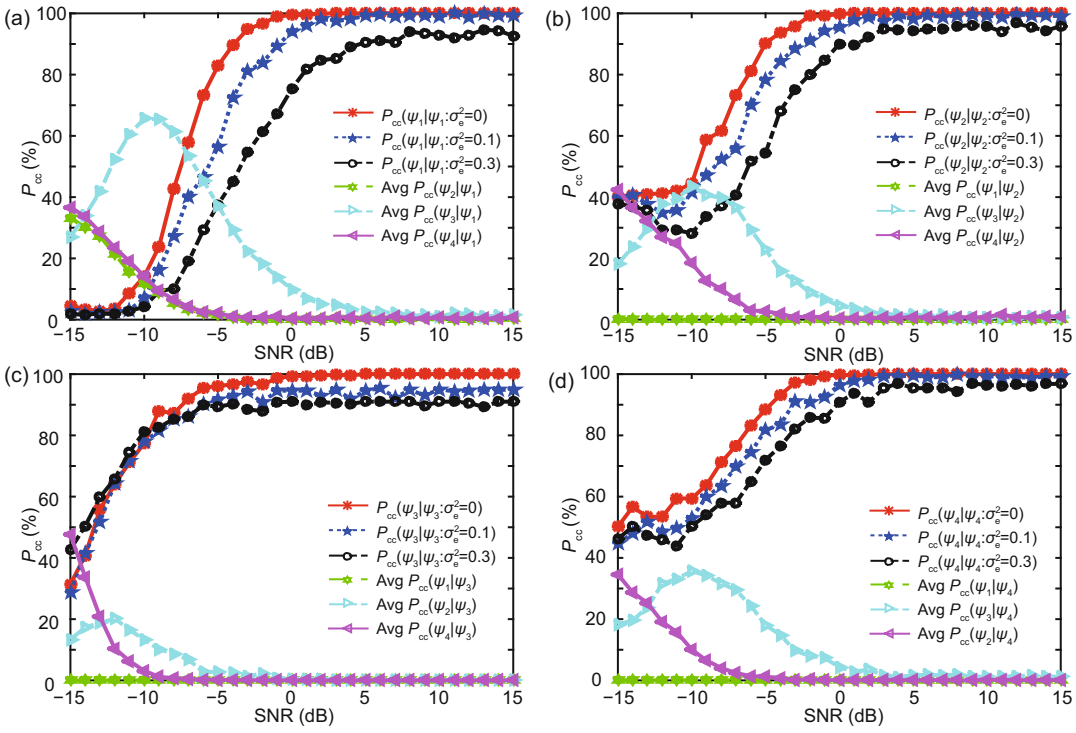

Fig. 3 Classification performance of 2×2 Al-STBC MIMO for $\psi_1 =$ BPSK (a), $\psi_2 =$ QPSK (b), $\psi_3 =$ 8PSK (c), and $\psi_4 =$ 16QAM (d) with $L = 1024$ symbols at different CSI estimation error values σ_e^2

6 Discussion and future work

For all the modulation hypotheses in the three scenarios discussed above, considerably high classification results were achieved even at CSI estimation error variance $\sigma_e^2 = 0.3$, which has not been reported in the literature to the best of our knowledge. Confusion matrices of all the three configurations, 2×1, 2×2, and 4×4, for σ_e^2=0, 0.1, and 0.3 at 0 dB SNR, are provided in Table 3. It is evident that in the case of perfect CSI ($\sigma_e^2 = 0$), 2×2 and 4×4 MIMO configurations exhibited perfect classification results. However, for the 2×1 MISO configuration, more than 90% correct classification was achieved. From Table 3, we can observe that for the 2×1 MISO configuration at $\sigma_e^2 = 0.3$, BPSK was falsely classified as 8PSK and 16QAM for about 20% and 15% of the instances, respectively. Similarly, when $\sigma_e^2 = 0.3$, BPSK had the lowest classification accuracy of 78% for the 2×2 configuration. It was falsely classified as

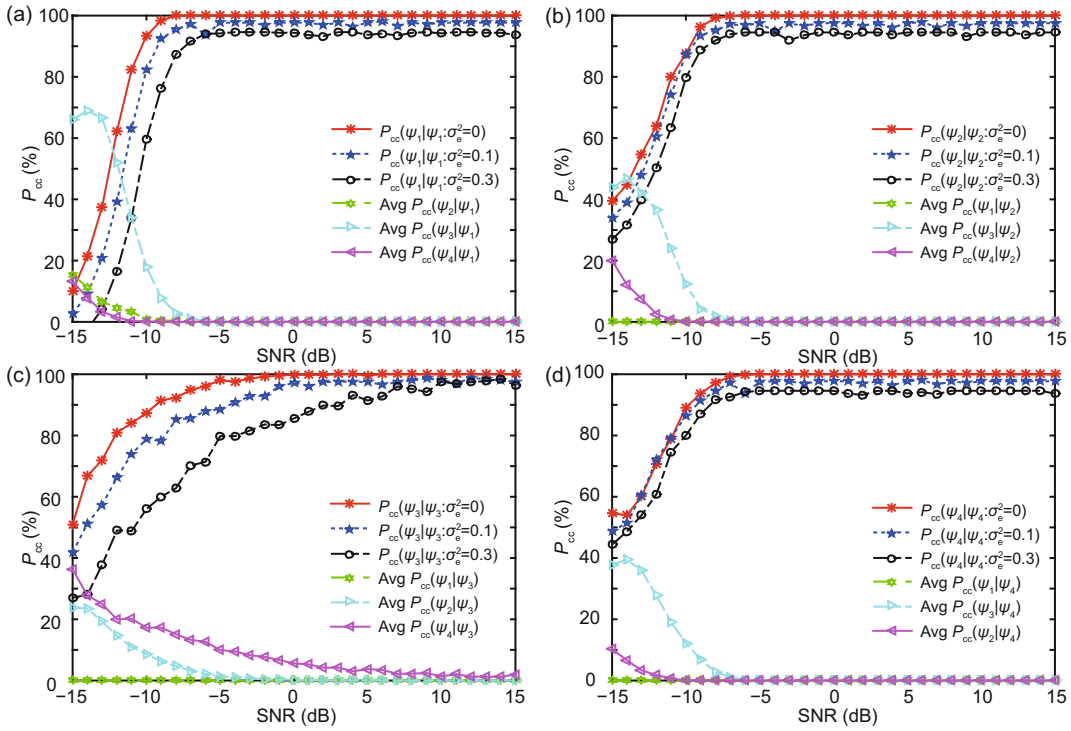

Fig. 4 Classification performance of 4×4 STTD-OTD MIMO for ψ_1 = BPSK (a), ψ_2 = QPSK (b), ψ_3 = 8PSK (c), and ψ_4 = 16QAM (d) with $L = 1024$ symbols at different CSI estimation error values σ_e^2

Table 3 Confusion matrices for 2×1, 2×2, and 4×4 configurations at $\sigma_e^2 = \{0, 0.1, 0.3\}$ with 0 dB SNR

Configuration		$\sigma_e^2 = 0$				$\sigma_e^2 = 0.1$				$\sigma_e^2 = 0.3$			
		BPSK	QPSK	8PSK	16QAM	BPSK	QPSK	8PSK	16QAM	BPSK	QPSK	8PSK	16QAM
2×1 MISO	BPSK	88	1	8	3	70	6	15	9	56	9	20	15
	QSPK	2	90	6	2	4	78	10	8	8	60	18	14
	8PSK	0	1	98	1	0	5	91	4	4	4	88	4
	16QAM	1	1	7	91	3	6	9	82	7	11	13	69
2×2 MIMO	BPSK	100	0	0	0	96	0	4	0	78	5	8	7
	QSPK	0	100	0	0	0	95	3	2	2	90	7	1
	8PSK	0	0	100	0	1	2	95	2	1	3	91	5
	16QAM	0	0	0	100	0	2	4	94	2	1	7	90
4×4 MIMO	BPSK	100	0	0	0	98	2	0	0	96	1	3	0
	QSPK	0	100	0	0	0	98	0	2	1	94	3	1
	8PSK	0	0	100	0	4	0	97	2	2	5	85	8
	16QAM	0	0	0	100	0	1	2	97	1	2	2	95

QPSK, 8PSK, and 16QAM for 5%, 8%, and 7% of the trials, respectively. When $\sigma_e^2 = 0.1$, 95% and 97.5% correct classifications were achieved in the cases of 2×2 and 4×4 configurations, respectively. Similarly, an average of 92.5% correct classification was achieved for the 4×4 configuration at 0 dB SNR and $\sigma_e^2 = 0.3$.

Table 4 gives a brief comparison of our proposed approach with some state-of-the-art AMC methodologies for MIMO systems. Although the underlying assumptions and MIMO system configurations may vary among each of the referred articles, they can still provide a fair comparison in terms of average classification accuracy. For instance, Choqueuse et al. (2009) used ALRT to tackle modulation classification in the MIMO system with a 2×4 configuration without perfect CSI. However, channel estimation error variance σ_e^2 was not provided. Choqueuse et al. (2009) achieved an average classification accuracy of 93% for the unknown channel scenario and around 98% in the case of perfect channel knowledge.

In Hassan et al. (2012), higher-order statistical moments and cumulants were used, and about 75% classification accuracy was achieved at 5 dB SNR and $\sigma_e^2 = 0.1$. In Turan et al. (2016), a joint probability distribution function was proposed for unknown antenna numbers and modulation type. However, it gave classification results with perfect channel knowledge only, i.e., 90% classification accuracy on average at 0 dB SNR. Luo et al. (2012) used an ML-based approach with a 2×3 antenna configuration and achieved about 93% classification accuracy on average at 0 dB SNR without perfect channel knowledge. However, the estimation error was not provided in this study. In Mühlhaus et al. (2012), fourth-order cumulants were used as the feature space for classification. An average classification accuracy of 94% was achieved without perfect CSI knowledge.

Table 4 Comparison of the proposed approach with the state-of-the-art methodologies with 0 dB SNR and imperfect CSI

Literature	Basic approach	$N_t \times N_r$	P_{cc}
Choqueuse et al. (2009)	ML-based	2×4	93.0%
Hassan et al. (2012)	Feature-based	2×4	75.0%
Turan et al. (2016)	ML-based	2×4	90.0%
Luo et al. (2012)	ML-based	2×3	93.0%
Mühlhaus et al. (2012)	Feature-based	2×4	94.0%
This paper	ML-based	4×4	97.5%

The methodology proposed in this study achieved an average accuracy of about 97.5% at 0 dB SNR with a channel estimation error variance of $\sigma_e^2 = 0.1$ for a 4×4 STBC-MIMO configuration. Complexity analysis for ML-based schemes was carried out in Section 4, and the approach proposed in this study provided the least complex solution among the ML candidates to the best of our knowledge. A detailed summary of state-of-the-art solutions based on ML and feature was given in Bahloul et al. (2016). However, most approaches deal with non-orthogonal MIMO systems for no more than two transmit antennas.

Based on the review in Section 1, AMC research for MIMO systems is still evolving and there are certain avenues which need further exploration. There are some aspects that we intend to tackle as part of our future research:

1. Use the potential of deep learning to tackle the problems of AMC in MIMO systems, where the number of transmit antennas is also unknown at the receiver.

2. Classify nonlinear modulations which are used in satellite communication such as minimum shift keying (MSK), Gaussian-MSK (GMSK), and Feher-patennted QPSK (FQPSK).

3. Expand the number of target modulations.

4. Work with signals received from the real environment for more realistic analysis.

7 Conclusions

A simple yet effective methodology has been proposed in this study to tackle the problems of AMC in STBC-MIMO systems. Using the ZF equalization technique, we modified the typical ALRT function for modulation classification of MIMO systems. The proposed ALRT function is independent of the number of antennas and the CSI matrix, and offers a considerably low-complexity likelihood solution for STBC-MIMO systems. Monte-Carlo simulations of 500 iterations for each hypothesis were carried out to verify the proposed approach. To the best of our knowledge, there has been no study which deals with modulation classification of STBC-MIMO for more than two antennas. Besides typical Al-STBC for 2×1 and 2×2 scenarios, we investigated the proposed approach for a 4×4 STBC-MIMO configuration. Moreover, the proposed approach has

been thoroughly investigated for blind channel scenarios with different values of the channel estimation error. Simulation results showed a promising classification outcome for a wide range of SNR and robust behavior against high CSI estimation error variance.

Compliance with ethics guidelines

Maqsood H. SHAH and Xiao-yu DANG declare that they have no conflict of interest.

References

Alamouti SM, 1998. A simple transmit diversity technique for wireless communication. *IEEE J Sel Areas Commun*, 16(8):1451-1458. https://doi.org/10.1109/49.730453

Ali A, Fan YY, 2017. Unsupervised feature learning and automatic modulation classification using deep learning model. *Phys Commun*, 25:75-84. https://doi.org/10.1016/j.phycom.2017.09.004

Aslam MW, Zhu ZC, Nandi AK, 2012. Automatic modulation classification using combination of genetic programming and KNN. *IEEE Trans Wirel Commun*, 11(8):2742-2750. https://doi.org/10.1109/TWC.2012.060412.110460

Bahloul MR, Yusoff MZ, Abdel-Aty AH, et al., 2016. Modulation classification for MIMO systems: state of the art and research directions. *Chaos Sol Fract*, 89:497-505. https://doi.org/10.1016/j.chaos.2016.02.029

Ben-Israel A, Greville TNE, 2003. Generalized Inverses: Theory and Applications. Springer, New York, USA.

Beres E, Adve R, 2007. Blind channel estimation for orthogonal STBC in MISO systems. *IEEE Trans Veh Technol*, 56(4):2042-2050. https://doi.org/10.1109/TVT.2007.897639

Choqueuse V, Azou S, Yao K, et al., 2009. Modulation recognition for MIMO communications. *Milit Tech Acad Rev*, 19(2):183-196.

Choqueuse V, Marazin M, Collin L, et al., 2010. Blind recognition of linear space-time block codes: a likelihood-based approach. *IEEE Trans Signal Process*, 58(3): 1290-1299. https://doi.org/10.1109/TSP.2009.2036062

Cormen TH, Leiserson CE, Rivest RL, et al., 2009. Introduction to Algorithms. MIT Press, Massachusettes, USA.

Courrieu P, 2008. Fast computation of Moore-Penrose inverse matrices. *Neur Inform Process Lett Rev*, 8(2):25-29.

Dobre OA, Abdi A, Bar-Ness Y, et al., 2007. Survey of automatic modulation classification techniques: classical approaches and new trends. *IET Commun*, 1(2):137-156. https://doi.org/10.1049/iet-com:20050176

Eldemerdash YA, Marey M, Dobre OA, et al., 2013. Fourth-order statistics for blind classification of spatial multiplexing and Alamouti space-time block code signals. *IEEE Trans Commun*, 61(6):2420-2431. https://doi.org/10.1109/TCOMM.2013.042313.120629

Hassan K, Nsiala Nzéza C, Berbineau M, et al., 2010. Blind modulation identification for MIMO systems. IEEE Global Telecommunications Conf, p.1-5.

Hassan K, Dayoub I, Hamouda W, et al., 2012. Blind digital modulation identification for spatially-correlated MIMO systems. *IEEE Trans Wirel Commun*, 11(2):683-693.

Huang CY, Polydoros A, 1995. Likelihood methods for MPSK modulation classification. *IEEE Trans Commun*, 43(2-4):1493-1504. https://doi.org/10.1109/26.380199

Jalloul LMA, Rohani K, Kuchi K, et al., 1999. Performance analysis of CDMA transmit diversity methods. 50th Vehicular Technology Conf, p.1326-1330. https://doi.org/10.1109/VETECF.1999.801478

Le Gall F, 2016. Solving Laplacian systems in logarithmic space. https://arxiv.org/abs/1608.01426

Luo MG, Li LP, Tang B, 2012. A blind modulation recognition algorithm suitable for MIMO-STBC systems. IEEE 12th Int Conf on Computer and Information Technology, p.271-276. https://doi.org/10.1109/CIT.2012.77

Marey M, Dobre OA, 2015. Blind modulation classification for Alamouti STBC system with transmission impairments. *IEEE Wirel Commun Lett*, 4(5):521-524. https://doi.org/10.1109/LWC.2015.2451174

Mühlhaus MS, Öner M, Dobre OA, et al., 2012. Automatic modulation classification for MIMO systems using fourth-order cumulants. IEEE Vehicular Technology Conf, p.1-5. https://doi.org/10.1109/VTCFall.2012.6399061

Nandi AK, Azzouz EE, 1997. Modulation recognition using artificial neural networks. *Signal Process*, 56(2):165-175. https://doi.org/10.1016/S0165-1684(96)00165-X

Nandi AK, Azzouz EE, 1998. Algorithms for automatic modulation recognition of communication signals. *IEEE Trans Commun*, 46(4):431-436. https://doi.org/10.1109/26.664294

Niu MB, Cheng JL, Holzman JF, 2014. Alamouti-type STBC for atmospheric optical communication using coherent detection. *IEEE Photon J*, 6(1):7900217. https://doi.org/10.1109/JPHOT.2014.2302807

Quan Z, Ribeiro MV, 2011. A low cost STBC-OFDM system with improved reliability for power line communications. IEEE Int Symp on Power Line Communications and Its Applications, p.261-266. https://doi.org/10.1109/ISPLC.2011.5764404

Salam AOA, Sheriff RE, Al-Araji SR, et al., 2015. Automatic modulation classification in cognitive radio using multiple antennas and maximum-likelihood techniques. 15th Int Conf on Computer and Information Technology, p.1-5. https://doi.org/10.1109/cit/iucc/dasc/picom.2015.3

Saurabh N, 2015. Improving the Performance of Moore-Penrose Pseudo-Inverse for a Graph's Laplacian Using GPU. MS Thesis, Amsterdam, the Netherlands. https://doi.org/10.13140/2.1.4457.5048

Shi M, Bar-Ness Y, Su W, 2007. STC and BLAST MIMO modulation recognition. IEEE Global Telecommunications Conf, p.3034-3039. https://doi.org/10.1109/GLOCOM.2007.575

Sills JA, 1999. Maximum-likelihood modulation classification for PSK/QAM. Military Communications Conf, p.217-220. https://doi.org/10.1109/MILCOM.1999.822675

Swami A, Sadler BM, 2000. Hierarchical digital modulation classification using cumulants. *IEEE Trans Commun*, 48(3):416-429. https://doi.org/10.1109/26.837045

Tarokh V, Jafarkhani H, Calderbank AR, 1999. Space-time block codes from orthogonal designs. *IEEE Trans Inform Theory*, 45(5):1456-1467. https://doi.org/10.1109/18.771146

Thao PC, Le Khoa D, Tu NT, et al., 2016. Optical MIMO DCO-OFDM wireless communication systems using STBC in diffuse fading channels. Proc 3rd National Foundation for Science and Technology Development Conf on Information and Computer Science, p.141-146. https://doi.org/10.1109/NICS.2016.7725639

Tseng SM, Liao CY, 2014. Distributed orthogonal and quasi-orthogonal space-time block code with embedded AAF/DAF matrix elements in wireless relay networks with four relays. *Wirel Pers Commun*, 75(2):1187-1198. https://doi.org/10.1007/s11277-013-1415-2

Tseng SM, Lee TL, Ho YC, et al., 2017. Distributed space-time block codes with embedded adaptive AAF/DAF elements and opportunistic listening for multihop power line communication networks. *Int J Commun Syst*, 30(1):e2950. https://doi.org/10.1002/dac.2950

Turan M, Öner M, Çırpan HA, 2016. Joint modulation classification and antenna number detection for MIMO systems. *IEEE Commun Lett*, 20(1):193-196. https://doi.org/10.1109/LCOMM.2015.2500898

Veljovic Z, Urosevic U, 2017. New solutions for cooperative relaying implementation of OSTBC with 3/4 code rate. *Wirel Pers Commun*, 92(1):51-61. https://doi.org/10.1007/s11277-016-3838-z

Wei W, Mendel JM, 2000. Maximum-likelihood classification for digital amplitude-phase modulations. *IEEE Trans Commun*, 48(2):189-193. https://doi.org/10.1109/26.823550

Zhu ZC, Aslam MW, Nandi AK, 2011. Support vector machine assisted genetic programming for MQAM classification. Int Symp on Signals, Circuits and Systems, p.1-6. https://doi.org/10.1109/ISSCS.2011.5978654